Spin fluctuations in a two-dimensional marginal Fermi liquid

P. B. Littlewood, J. Zaanen, and G. Aeppli
AT&T Bell Laboratories, Murray Hill, New Jersey 07974

H. Monien
Institute for Theoretical Physics, University of California, Santa Barbara, California 93106
(Received 21 December 1992)

We use a simple two-dimensional band-structure model for $La_{2-x}Sr_xCuO_4$ incorporating marginal-Fermi-liquid self-energy corrections to calculate the spin-fluctuation spectrum at low energies. Features in the band structure lead to peaks in the structure factor at incommensurate wave vectors. The frequency and temperature dependence of these peaks is controlled by the quasiparticle lifetimes. Comparison with both neutron-scattering data and NMR or NQR relaxation rates suggests a modest mass enhancement, and indicates neither strong magnetic-exchange interactions nor a separate non-Fermi-surface contribution to the polarizability. We compare our results with conventional Fermi-liquid behavior, and with a model of magnetic fluctuations with a long correlation length.

I. INTRODUCTION

Since the insulating parents of the high-temperature cuprate superconductors are localized antiferromagnets (AF), the quest for magnetic fluctuations in the metallic phases has been aggressively pursued. The strongest indication that AF fluctuations persist in the superconducting phases has come from nuclear-magnetic-resonance (NMR) relaxation rate measurements which show T_1^{-1} enhanced over the band-structure value for the planar Cu site with unusual temperature dependence,[1] while the corresponding planar O follows a modified Korringa relationship $(T_1T)^{-1} \propto K_s$ in $YBa_2Cu_3O_7$.[2] Within a model where the dominant hyperfine interactions are transferred from near neighbors,[3,4] these results suggest commensurate AF fluctuations with a long, and temperature-dependent, correlation length.[5,6]

NMR measures the local spin fluctuations and therefore averages the structure factor over reciprocal space. A clearer picture of the magnetic structure factor $S(\mathbf{q},\omega)=[1+n(\omega)]\chi''(\mathbf{q},\omega)$ is now emerging from inelastic neutron-scattering measurements on $La_{1.95}Ba_{0.05}CuO_4$,[7,8] $La_{2-x}Sr_xCuO_4$,[9,10] and metallic superconducting samples of $YBa_2Cu_3O_{7-x}$.[11] Most dramatic is the observation of sharp, incommensurate peaks in $La_{2-x}Sr_xCuO_4$, with a spectral weight comparable to that associated with spin waves in the insulating parent; the peak widths are unusually ω and T dependent.[10]

Turning aside from the magnetic response, a different perspective on these materials is obtained by focusing on the quasiparticle properties. The photoemission[12] and positron annihilation results[13] have for $YBa_2Cu_3O_7$ and $Bi_2Sr_2CaCu_2O_8$, established the existence of a Fermi edge whose position is close to that predicted from band structure. However, the quasiparticle linewidth grows rapidly with energy away from E_F.[14] The "marginal-Fermi-liquid"[15,16] scenario of a quasiparticle scattering rate *linear* in frequency or temperature (whichever is greatest) in fact provides a consistent description of photoemission, the linear bias dependence of the tunneling conductance, infrared absorption, and electronic Raman scattering.[17] It was suggested that such an anomalous self-energy could be obtained by the interaction of quasiparticles with a particle-hole pair spectrum of the form $F(\mathbf{q})\tanh(\omega/T)$.[15] Thus both the polarizability and the self-energy would be logarithmically singular in the limit $\omega, T \to 0$. Since the optical response tests only the $q \to 0$ limit, where the continuity equation rules out any singular contribution to the charge or spin-density response,[16] such a singular *local* polarizability is expected to be visible only in finite-q probes (in the spin channel NMR and neutron scattering). Nevertheless, nothing in the original picture suggested that the singular response would be confined to a narrow region of momentum space.

Nevertheless, the success of the marginal-Fermi-liquid (MFL) phenomenology in describing both transport and single-particle properties suggests that the heavily doped compounds are amenable to a bandlike picture. Whether or not interactions between the quasiparticles can give rise to a singular local polarizability, there must at least be a "conventional" contribution to the susceptibility analogous to the Lindhard response function of the free Fermi gas. It is that contribution that we work out here.[18] We shall argue that (i) the peaks seen in neutron scattering are produced by simple Fermi-surface effects in an itinerant model and (ii) more importantly, their (ω, T) dependence can be reproduced by a finite quasiparticle lifetime consistent with the model of a marginal Fermi liquid.[15] We thus obtain a reconciliation of the MFL

phenomenology, originally developed to describe long-wavelength properties, with the short length-scale structure seen in NMR and neutron scattering.

We are of course not alone in noting that Fermi-surface nesting features will give rise to incommensurate peaks in χ [point (i) above].[19–24] Lu *et al.*[23] have noted that even without nesting, in *two* dimensions any Fermi-liquid-like model will give singular momentum dependence of $\mathrm{Im}[\chi(q\to 2k_F,\omega\to 0)]=\chi''$.[25] If nesting effects are weak, there will be little enhancement of $\mathrm{Re}[\chi(\mathbf{q},0)]$. However, a free Fermi gas description will fail badly to describe the energy and temperature dependence observed in experiment; the characteristic scale is the Fermi energy.[26] We believe that the MFL approach provides a natural explanation for the energy and temperature dependence by broadening the Fermi-surface singularities because of quasiparticle lifetime. We find no need to invoke strong magnetic interactions.

We stress, however, that the itinerant model we adopt should not be taken to imply consistency with local-density approximation (LDA) band-structure models. We find evidence of significant band narrowing in comparison to LDA ($m^*/m_b\sim 2-4$). The LDA bands have considerably more three-dimensional character than is consistent with the measured anisotropy of the resistivity and plasma frequency[27] with our interpretation of neutron-scattering measurements.

There are two principal contributors to the result we shall present. The momentum dependence is almost entirely determined by the spectral details of the band structure. However, the energy and temperature dependence is produced principally by the self-energy, at least for low-energy transfers in the range of momenta where $\chi''(\mathbf{q},\omega)$ is large. We shall first present the model and calculations, and then engage in comparison with data on $La_{2-x}Sr_xCuO_4$ and give some discussion of the properties of other cuprates.

II. MODEL AND CALCULATIONS

A. Dynamical susceptibility

We wish to calculate the dynamical susceptibility

$$\chi(\mathbf{q},\omega)=\frac{2\mu_b^2}{N}\sum_{\mathbf{p}}\int\frac{d\nu}{2\pi}\int\frac{d\nu'}{2\pi}\Lambda(\mathbf{p},\nu;\mathbf{p}+\mathbf{q},\nu')\frac{A(\mathbf{p},\nu)A(\mathbf{p}+\mathbf{q},\nu')}{\nu-\nu'+\omega+i\delta}[f(\nu')-f(\nu)]\ , \tag{1}$$

where $f(\nu)$ is the Fermi occupation factor, and

$$\begin{aligned}A(\mathbf{p},\nu)&=-2\,\mathrm{Im}[G(\mathbf{p},\nu)]\\&=-2\,\mathrm{Im}[\nu-\varepsilon(\mathbf{p})-\Sigma(\mathbf{p},\nu)]^{-1}\ ,\end{aligned} \tag{2}$$

is the electron spectral function, $\varepsilon(\mathbf{p})$ the conduction-band energy, and Σ the electron self-energy. Λ is a vertex function representing the effect of interactions within the excited particle-hole pair. If strong AF couplings are present, it will be peaked near $\mathbf{q}=(\pi,\pi)$. We show below that the Fermi-surface contribution to Eq. (1) has sufficient structure to account for the neutron-scattering data. Thus, we set $\Lambda=1$, because if not a strong function of momentum, its effects on our calculation are indistinguishable from a mass (bandwidth) renormalization. Estimates from optical data[15] suggest that $\Lambda\sim 2$ at temperatures near T_c. For the MFL self-energy, we adopt a simple analytic form[15]

$$\Sigma=\pi\lambda[(2\omega/\pi)\ln([T+i\omega]/\omega_c)+iT]\ .$$

We note that $\lim_{T\to 0}\lim_{\omega\to 0}\chi''(\mathbf{q},\omega)/\omega$ is a Fermi-surface quantity and is unaffected by purely energy-dependent self-energy corrections, as in the MFL hypothesis. At nonzero temperature or frequency there are considerable differences, which we detail below.

Before we go into the detailed calculation incorporating both band-structure and lifetime effects, it is instructive to remind ourselves of the result for a *free* electron gas. In two dimensions $\lim_{T\to 0}\lim_{\omega\to 0}\chi''(\mathbf{q},\omega)/\omega$ is singular for any $\mathbf{q}$ such that the Fermi surface (FS) is mutually *tangential* (but not necessarily nested) to the FS displaced by $\mathbf{q}$. For example, in two-dimensional free-electron gas (parabolic bands), we have the familiar (Lindhard) result

$$\lim_{\omega\to 0}\chi_L''(\mathbf{q},\omega)/\omega=(4qk_F)^{-1}(1-q^2/4k_F^2)^{-1/2}\Theta(2k_F-q)\ , \tag{3}$$

with a square-root singularity at $2k_F$ which will be cutoff by the quasiparticle decay rate $\mathrm{Im}(\Sigma)$ [$\propto\max(\omega,T)$ in MFL]. Without additional FS nesting, there is no corresponding peak in $\mathrm{Re}[\chi(\mathbf{q},\omega)]$. This line of singularities will cut the zone boundary close to (π/π) in the cuprates; band-structure effects, in particular the strength of Umklapp scattering, will determine the details. The q dependence, and doping dependence of $\chi''(\mathbf{q},\omega)$ can be qualitatively described by inscribing circles of radius $2k_F$ about the reciprocal lattice vectors. For dopings somewhat below half-filling, these will intersect at four points on the zone boundary $\pi(1\pm\delta Q,1)$, $\pi(1,1\pm\delta Q)$ (see Fig. 1). At these points, we then expect to see peaks in $\chi''(\mathbf{q},\omega)$.

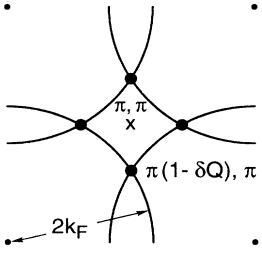

FIG. 1. Schematic picture of the evolution of Fermi-surface singularities in a band-structure model for $La_{2-x}Sr_xCuO_4$.

With a more realistic band-structure model, this picture needs some small modifications.

B. Model band structure

For our purposes, we need a good description of the dispersion near the Fermi surface, describing accurately the band effective mass, the doping level of the Van Hove singularity, and the curvature of the Fermi surface. The appropriate values of these parameters are not known with great accuracy, even if one believes the LDA band structure provides a correct description of the dispersion. We model the Fermi surface with a three-band Hamiltonian comprising hybridized Cu $d_{x^2-y^2}$ and O p_x and p_y orbitals:

$$H_0=\varepsilon\sum_i (c_{di}^\dagger c_{di}-c_{xi}^\dagger c_{xi}-c_{yi}^\dagger c_{yi}) + \sum_{ij}[t_{ij}c_{di}^\dagger c_{xy}+\text{H.c.}+(x\rightarrow y)] + \sum_{ij}[t'_{ij}c_{xi}^\dagger c_{xj}+\text{H.c.}]\ . \quad (4)$$

Here $\varepsilon=\frac{1}{2}(E_d-E_p)$ and we have included a nearest-neighbor Cu-O hybridization $t_{ij}=\pm t$, and O(p_x)-O(p_y) hybridization $t'_{ij}=\pm t'$. The O-O hopping breaks the special symmetries which obtain at half-filling for a simple one-band model with nearest-neighbor coupling. With $t'=0$, the Fermi surface at half-filling is square and there is thus perfect nesting of the FS under a displacement (π,π); coincident with half-filling is a Van Hove singularity in the density of states. The use of a three-band model is not crucial, as there is only a single band near the Fermi surface; for us it provides the advantage of a basis in which to calculate the NMR relaxation rates for different nuclei.

In Fig. 2, we show the Fermi surface at different values of filling for the parameters $\varepsilon=1.2$ eV, $t=-1.5$ eV, and $t'=0.5$ eV, which are good fits of a three-band model to LAPW band structure over a range of several eV near the Fermi surface. At low density (large x), the FS is electronlike, but as the electron filling is increased (reducing x) the FS becomes increasingly square; at a doping x_{sq}, the curvature of the FS changes sign around the FS, with the "holelike" pieces growing. Finally, as doping is reduced through the Van Hove singularity, at x_{vh} the FS becomes entirely holelike. So for fillings $x_{vh}<x<x_{sq}$, there are two values of Q along the zone face that satisfy the "touching" condition, where the low-frequency imaginary susceptibility will be singular. The values of δQ (measured from the zone corner, see Fig. 1) are plotted in Fig. 3 as a function of doping (measured from x_{vh} for several different values of t'. In practice, we shall see that the singularity nearest the zone corner (i.e., smallest δQ) has the largest amplitude and dominates the response. Note also that the singularities are sharpest (smallest width in momentum space) at $x=x_{sq}$, since this marks the doping level of strongest nesting. δQ is generally larger than in the square lattice single-orbital model (i.e., $t'=0$) and closer to the typical values observed in experiment.

While the three-band model can give reasonable fit to the LDA band structure over several eV, it fails to place the Van Hove singularity at the same doping level as the LDA.[28] The doping level of the Van Hove singularity is determined by the band structure and density of states far from the Fermi level. Better agreement with LDA can be obtained by including hybridization with other bands (e.g., Cu 4s), which have a tendency to compress the $d_{x^2-y^2}$-p manifold. However, it is not necessarily appropriate to make a detailed fit to LDA because the properties of the itinerant carriers are probably very strong re-

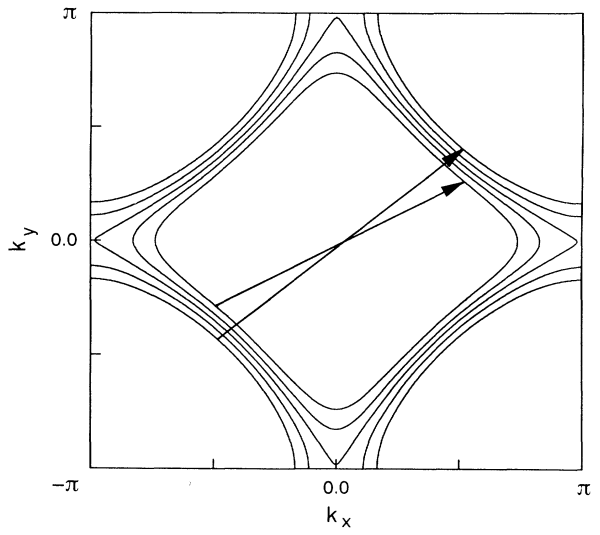

FIG. 2. Fermi surface at different doping levels $x-x_{vh}=-0.10$, -0.05, 0.00, 0.05, and 0.12 for $\varepsilon=1.2$ eV, $t=-1.5$ eV, and $t'=0.5$ eV. The arrows mark the direction of "best" nesting.

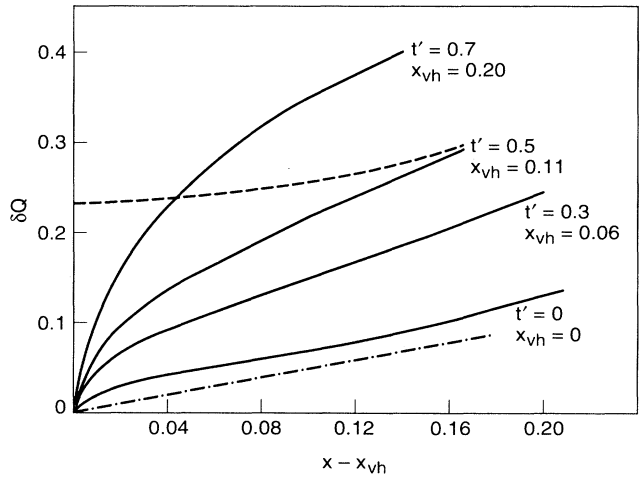

FIG. 3. Position of dominant peaks in $\chi''(\mathbf{q},\omega\rightarrow 0)$, at $\mathbf{Q}_s=\pi(1-\delta Q,1)$ as a function of doping measured from x_{vh}, for $\varepsilon=1.2$ eV, $t=-1.5$ eV, and several values of t'. In the case of $t'=0.5$ eV only, the position of the secondary nesting peak is shown by the dashed line. The chain line is expected from a model of domain walls separating AF regions.

normalized from the LDA bands. In our case we shall use the three-band model simply to parametrize the band structure.

Since our results are strongly influenced by proximity to the Van Hove singularity, we choose a representative set of parameters, and measure the density away from x_{vh}. There are then three important measures of our band structure: (1) the value of x_{vh}, which determines the density at which $\delta Q \to 0$, and the peaks become commensurate, (2) the ratio t'/t, which determines the shape of the Fermi surface, and in particular the scale of δQ variation with x (see Fig. 3), and (3) the density of states near the Fermi level, which we shall for convenience parametrize by a rescaling of all the band parameters with an effective mass m^*.

The appropriate density of states can be estimated from the measured static Pauli susceptibility, which is free from MFL renormalization.[29] Using the canonical parameters of Fig. 2, we calculate $\chi'(\mathbf{0},0)/\mu_B^2 = 1(\text{eV-Cu})^{-1}$ at $x \sim 0$ (i.e., away from Van Hove singularity). The LAPW band structure gives a value of $\sim 2\ \text{eV}^{-1}$,[28] still smaller than experimental estimates of the Pauli susceptibility of $\sim 4\ (\text{eV-Cu})^{-1}$.[30] Thus we require a modest mass enhancement $m^* \sim 5$, only about half of which arises from many body corrections beyond LDA. This mass correction affects only the local susceptibility, and does not enhance special regions of $\mathbf{q}$. In the rest of this paper, we shall present results for $\varepsilon = 1.2$ eV, $t = -1.5$ eV, $t' = 0.5$ eV, and $m^* = 5$. Aside from changes of scale, all our results are qualitatively similar when expressed as a function of $x - x_{vh}$.

III. RESULTS

A. Spin susceptibility

Figure 4 shows $\chi''(\mathbf{q},\omega)$ calculated from our model at low frequency and temperature ($\omega = 2$ meV, $T = 4$ meV), for four different values of doping. In addition we have included the MFL self-energy with $\lambda = 0.3$, $\omega_c = 1$ eV, parameters taken from approximate fits to optical and resistivity data.[15] At this low temperature and frequency, the self-energy corrections are not large. We have restricted the region plotted to a quarter of the zone near π, π—i.e., $\pi/2 < q_x, q_y < 3\pi/2$. The ridges in the figure are lines of singularities, due to FS touching, which we have

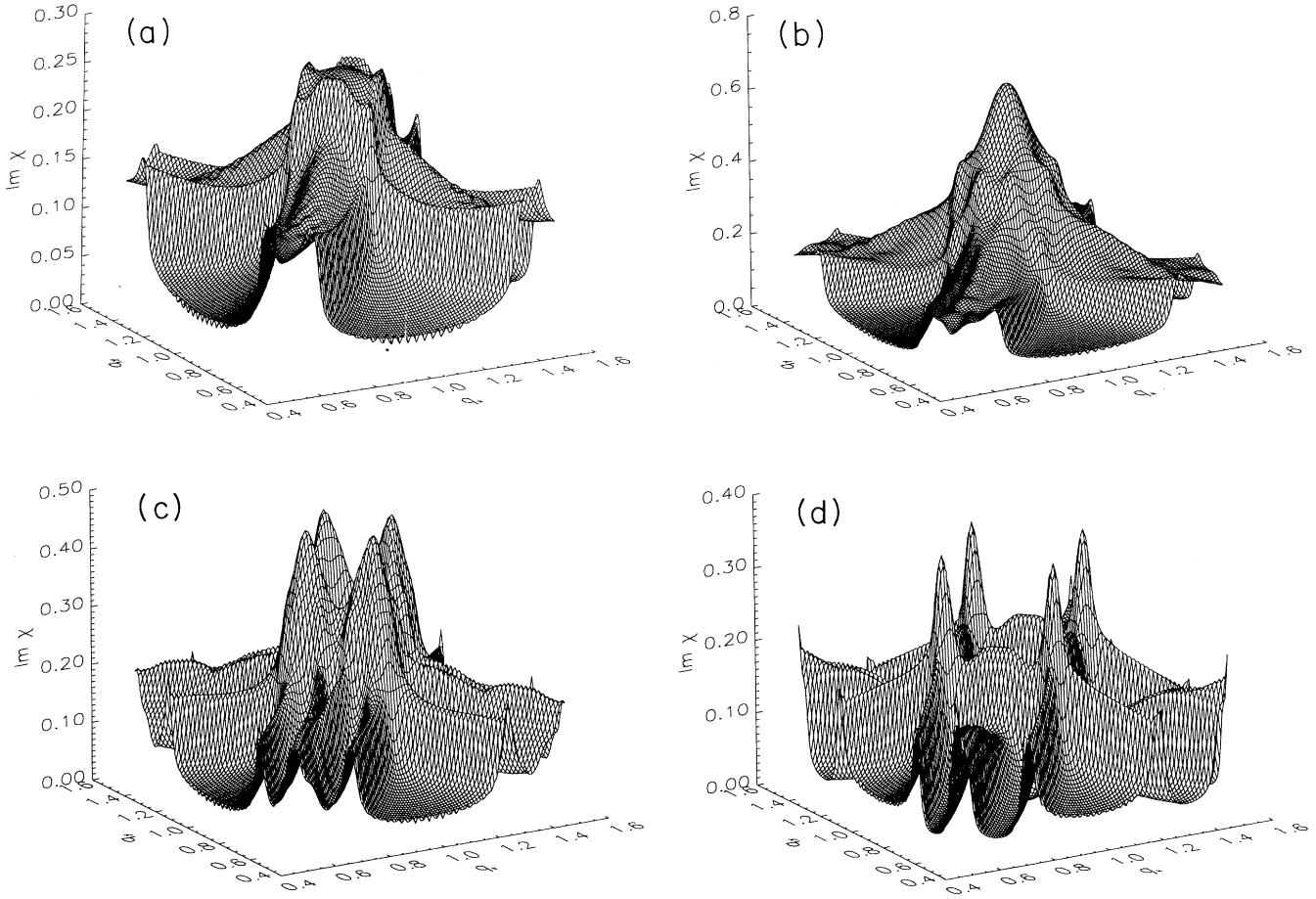

FIG. 4. Perspective plot of $\text{Im}[\chi(\mathbf{q},\omega = 2\ \text{meV})]/\mu_B^2$ convoluted with a Gaussian broadening (see text) for $\varepsilon = 1.2$ eV, $t = -1.5$ eV, $t' = 0.5$ eV, $\lambda = 0.3$, $\omega_c = 1$ eV, $T = 2$ meV, and $m^* = 5$. Contour labels are values in $(\text{eV})^{-1}$. The dashed lines mark lines of singularities for FS "touching". Doping levels are $x - x_{vh} = -0.04$ (a); 0.01 (b); 0.06 (c); 0.12 (d).

broadened by convolution with a Gaussian of width $0.01\pi/a$ (comparable to experimental resolution[10]). For $x < x_{vh}$, we find a broad peak at (π,π); although this peak does not correspond to $2k_F$, and it is not therefore singular, it has the dominant spectral weight. For doping levels beyond x_{vh}, the peak splits into four and *sharpens*. These results are primarily a measure of Fermi-surface geometry, and are thus qualitatively similar to the calculations of others.[20,23,25] Away from the ridges and peaks, the value of $\chi''(\mathbf{q},\omega)$ is very small.

At fillings where the curvature of the FS changes sign as a function of angle, the topology of touching FS becomes quite complex; then there are *two* singular points along the zone face, and hence in principle eight peaks in $\chi''(\mathbf{q},\omega)$ near (π,π) (see Fig. 3). In practice the subsidiary peaks are not resolved due to inelastic effects in our calculations (see below); they produce, for example the unusual "square" line shape in Fig. 4(a).[25] The peaks are sharpest at a doping when the two singular points converge (i.e., at $x = x_{sq}$, where the Fermi surface is "squarest") and broadest near the Van Hove singularity, and closer to half-filling.

It is important to recognize that the singular behavior in $\chi''(\mathbf{q},\omega)$ at low frequencies does not imply an enormous enhancement of the static susceptibility $\mathrm{Re}[\chi(\mathbf{q},\omega=0]$, which would indicate strong nesting. In Fig. 5 we plot the static susceptibility for the same parameters as Fig. 4 (in this case over the whole zone). The nesting features are evident, particularly at larger doping levels, but the enhancement over parabolic bands is not more than a factor of 3. Neither is there strong energy nor temperature dependence at the peaks—at the points in momentum space where $\mathrm{Im}[\chi(\mathbf{q},\omega)]/\omega$ is divergent as $\omega \to 0$, $\mathrm{Re}[\chi(\mathbf{q},\omega)]$ has a cusp.

While the existence of peaks in the structure factor at the appropriate values of momentum follow directly from the band-structure model, the energy and T dependence observed requires an explanation beyond simple band structure, which by itself would give rise to energy or temperature dependence only on scales comparable to the energy dependence of the joint density of states. The marginal-Fermi-liquid ansatz, which has been successful in explaining many anomalous properties of the cuprates, notably the single particle spectral functions $A(p,\nu)$ measured by tunneling and photoemission, again plays a natural role here, where we are dealing with an integral, Eq. (1), over the products of one-particle spectral functions. Since according to this ansatz,

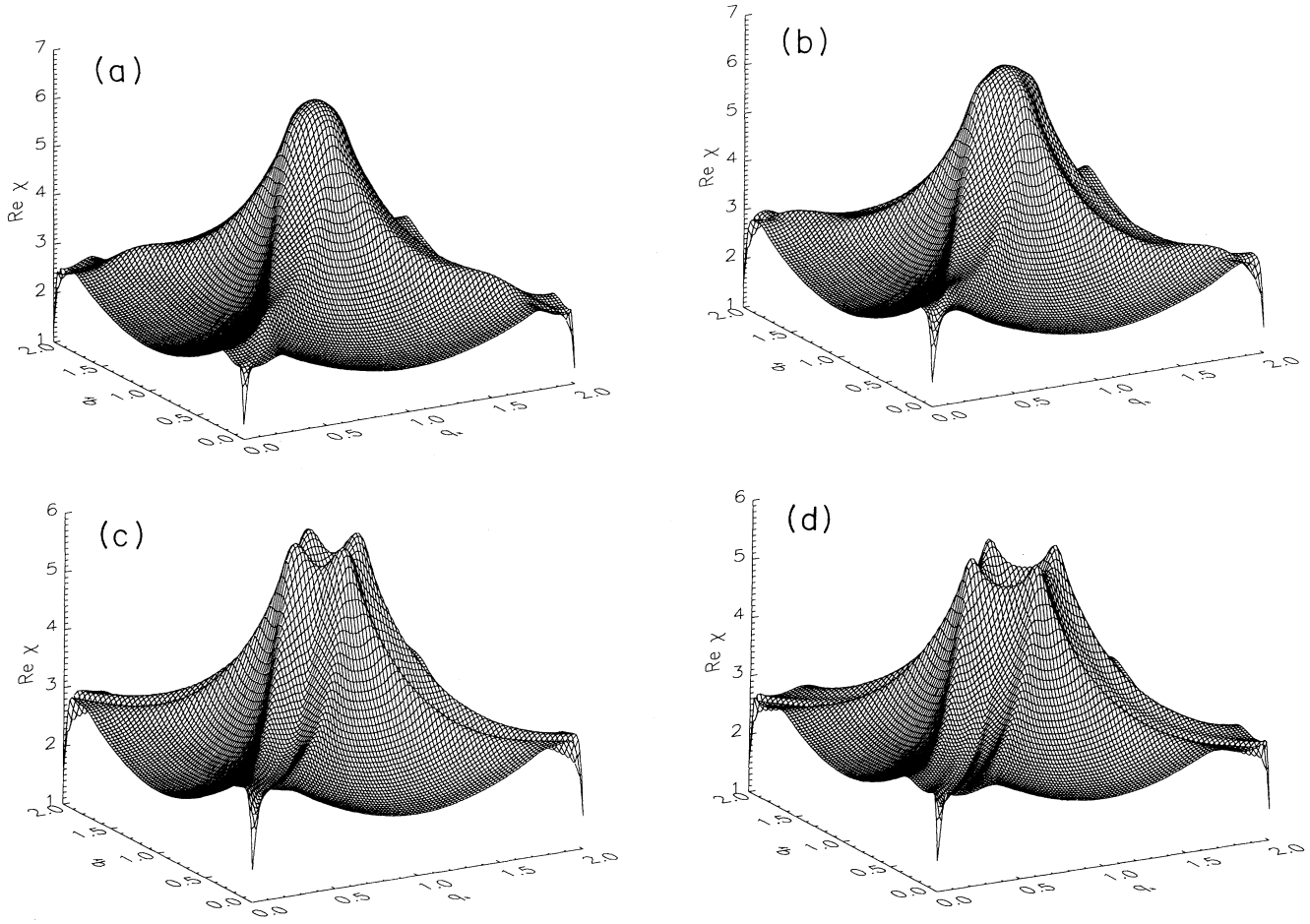

FIG. 5. Perspective plot of $\mathrm{Re}[\chi(\mathbf{q},\omega=0)]$ for the same parameters and doping levels as Figs. 4(a)–4(d).

$1/\tau \propto \mathrm{Im}(\Sigma) \propto \max(\omega, T)$, we expect that near $q = 2k_F$ the susceptibility becomes strongly temperature and frequency dependent. Explicit calculation bears this out, and in Fig. 6 we show $\chi''(\mathbf{q},\omega)$ calculated at low frequency $\omega = 2$ meV and higher temperatures $T = 10$ meV (a), 50 meV (b), as well as the low-temperature susceptibility at a larger energies $\omega = 20$ meV (c), 100 meV (d). The peaks are rapidly smoothed by going to either nonzero temperature or nonzero frequency on account of the rapid increase in the quasiparticle scattering rate with either ω or T.

In fact the smoothing is approximately the same with either ω or T (with a scale factor controlled by the crossover scale in the self energy—here set to π). This is shown explicitly in Fig. 7 where we present the calculated spectral function $S(q,\omega) = [1 + n(\omega)]\chi''(q,\omega)$ at a low temperature. While the overall behavior is rather complex, the value of the spectral function at the peak shows much less frequency and temperature dependence than expected from a Fermi liquid. The detailed balance factor approximately cancels the frequency dependence of χ'' at wave vectors near the peak(s), so that $S(\mathbf{Q}_{\mathrm{peak}},\omega)$ is flat. Near the peak(s) a crossover occurs on a scale $\omega \sim T$, but

$$\chi''(\mathbf{q} \sim \mathbf{Q}_{\mathrm{peak}}) \approx \omega/\Sigma''^{1/2} \approx \omega/\sqrt{\max(\omega, T)} \ .$$

This does not fit the simple functional form $F(\mathbf{q})\tanh(\omega/T)$ suggested theoretically[15] and found to agree with some experimental results.[7,8] Accidentally, this form works quite well as a fit to our results *at low doping* before the separated peaks are fully resolved. Experiment is more sensitive to the scale of the crossover than to any detailed functional dependence either at small or large ω. In a conventional Fermi liquid, S continues to grow linearly with frequency up to a scale of order the Fermi energy.

With doping, the line shape changes from a single rounded peak [Fig. 7(a)] which becomes first quite square [in Fig. 7(b) the two component peaks are unresolved] and then develops into two well-separated features [Figs. 7(c) and 7(d)]. For doping levels close to x_{vh} [Fig. 7(c)], the line shape evolves with frequency from two well-separated peaks into a single broad feature, while the maximum intensities show little frequency dependence. The broadening is asymmetric, with the region near (π,π) filling in with both increased frequency and temperature, in agreement with experiment.[7,10]

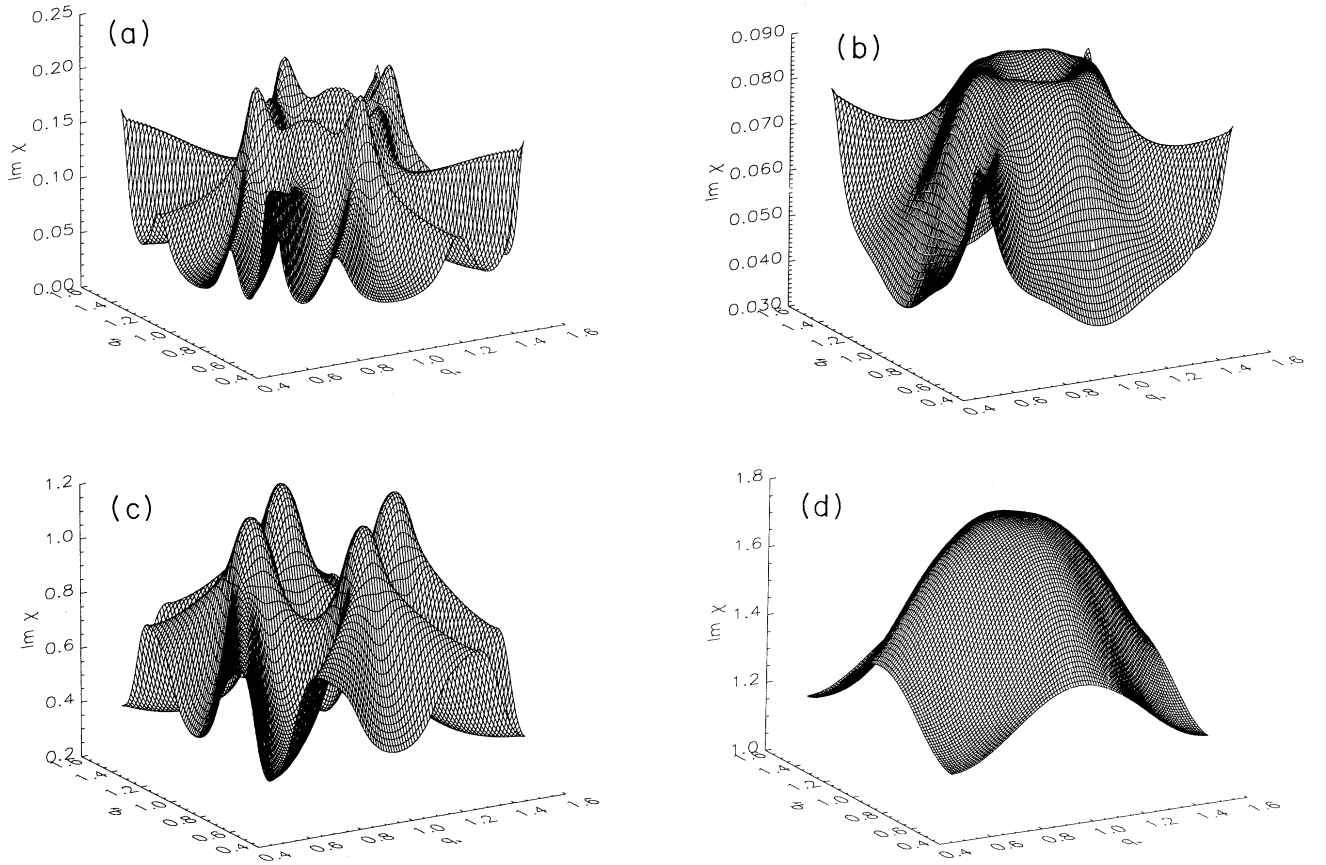

FIG. 6. Perspective plot of $\mathrm{Im}[\chi(\mathbf{q},\omega = 2\ \mathrm{meV})]/\mu_B^2$ for $\varepsilon = 1.2$ eV, $t = -1.5$ eV, $t' = 0.5$ eV, $\lambda = 0.3$, $\omega_c = 1$ eV, and $m^* = 5$. The same parameters as Figs. 4(d) and 5(d), but the following temperatures and frequencies (in meV). (a) $T = 10$, $\omega = 2$; (b) $T = 50$, $\omega = 2$; (c) $T = 2$, $\omega = 20$; (d) $T = 2$, $\omega = 100$.

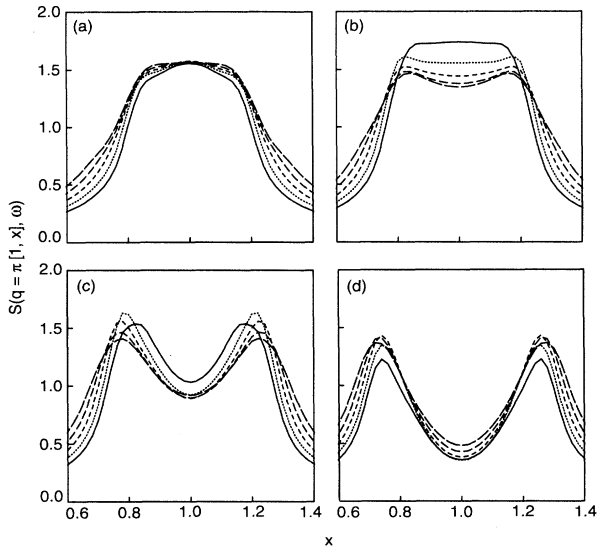

FIG. 7. Spectral function $S(\mathbf{q},\omega)$ along $\mathbf{q}=\pi(1,x)$ with same parameters as Figs. 4(a)–4(d), at $T=20$ K, and energies $\omega=3$ meV (solid line), 6 meV (dotted), 9, 12, and 15 meV (long dashed).

B. NMR relaxation rate

The strong temperature dependence of the susceptibility at low frequency is most clearly manifest in NMR relaxation, since T_1^{-1} is proportional to a weighted average of $\chi''(\mathbf{q},\omega)/\omega$ over the zone. Strong T dependence is only found in the vicinity of the touching singularities (i.e., $\mathbf{q}\sim Q_{\rm peak}$), which of course allows a different T dependence for Cu and O NMR relaxation rates. Following earlier work[3–6] the orbitals are coupled to the nuclei via the hyperfine Hamiltonian

$$H_{\rm nf}={}^{63}I_n[\,\mathbf{A}c^{\dagger}_{d\alpha}\sigma_{\alpha\beta}c_{d\beta}+Bc^{\dagger}_{4s\alpha}\sigma_{\alpha\beta}c_{4s\beta}\,] +C\,{}^{17}I_n(c^{\dagger}_{3s\alpha}\sigma_{\alpha\beta}c_{3s\beta})\,, \tag{5}$$

which includes (anisotropic) dipolar coupling of the Cu nucleus to $d_{x^2-y^2}$ orbitals, as well as an (isotropic) Fermi contact interaction to the Cu 4s or O 3s orbitals. We calculate the occupancy of the s orbitals within perturbation theory from overlap with neighboring orbitals, generating a transferred hyperfine coupling similar to that of Mila and Rice,[3] although we use band wave functions [i.e., a susceptibility from Eq. (2)], and not the ionic limit.[6] However we have found that the two approaches yield results differing only by factors ~ 2. From the Cu and O Knight shifts, we fix the parameters $A_{\parallel}$, B, and C; $A_{\perp}$ can be determined from the anisotropy of the Cu relaxation rate, leaving both[17] T_1 and ${}^{63}T_1$ as tests of the model. In contrast to the calculation of the susceptibility, the NMR calculations depend additionally on the basis wave functions, here obtained from our three-band model. Consequently, the failure to properly reproduce correlations embedded in the effective band structure (e.g., Zhang-Rice singlet formation) may invalidate our approach. However, because we use the Knight shifts to determine hyperfine coupling constants, dependence on any scale factors for the bandwidth (i.e., m^*) is removed.

There are no accurate measurements of the electronic component of the Knight shift in $La_{2-x}Sr_xCuO_4$. We have adjusted the hyperfine constants to provide values of the Knight shift comparable to those measured in $YBa_2Cu_3O_7$ (Ref. 31) (${}^{63}K_{\parallel}=0$, ${}^{63}K_{\perp}=0.003$, and ${}^{17}K=0.002$). We also assume that $A_{\perp}$ is small (for values, see Fig. 8). (Because the Knight shift depends on the $q=0$ susceptibility, we have used the unrenormalized static susceptibility to calculate K.) The weak temperature dependence of the calculated shifts (Fig. 8) thus has its origin in sharp features of the band structure. Calculated $(T_1T)^{-1}$ are shown in Fig. 9, again for the representative parameters of Figs. 4–6. The Cu relaxation rates are large and comparable to experimental values,[32] and more than an order of magnitude larger than ${}^{17}T_1^{-1}$; the numerical agreement would be less good using calculated values of the hyperfine coupling constants. We also find non-Korringa behavior for O, which would be expected on general grounds from an incommensurate peak in $S(\mathbf{q},\omega)$ and the conventional hyperfine Hamiltonian (5). Also the susceptibility is singular along lines throughout the Brillouin zone, and therefore always makes some contribution to any local susceptibility. Without the MFL self-energy corrections, the temperature dependence would be close to Korringa (i.e., $T_1^{-1}\propto T$) with small deviations due to the energy-dependent density of states.

We also note that any additional source of lifetime broadening for quasiparticles will change the results. The effect of adding an impurity scattering rate $\mathrm{Im}(\Sigma)=\tau_0^{-1}$ will be to drive the low-T behavior more Korringa-like

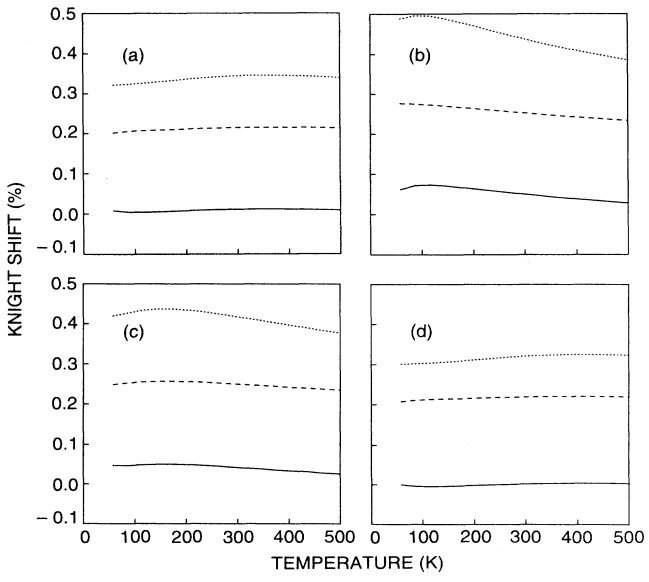

FIG. 8. Calculated Knight shifts (%) for hyperfine constants $A_{\perp}=0$, $A_{\parallel}=-3\times10^{-5}$, $B=5\times10^{-6}$, and $C=8\times10^{-6}$, for the same parameters as Fig. 4(a)–4(d). Solid line ${}^{63}K_{\parallel}$; dotted line ${}^{63}K_{\perp}$; dotted line ${}^{17}K$.

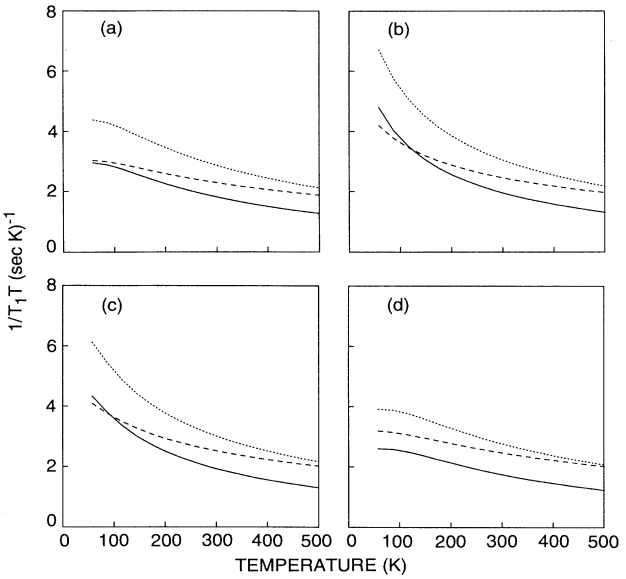

FIG. 9. Calculated NMR relaxation rates $(T_1T)^{-1}$ corresponding to the hyperfine coupling constants in Fig. 8. Band parameters are the same as Figure 4(a)–4(d). Solid line $(^{63}T_1^{-1})_{\|}$; dotted line $(^{63}T_1^{-1})_{\perp}$; dotted line $^{17}T_1^{-1}\times 10$. Note that the oxygen relaxation rate has been scaled by a factor of 10.

for temperatures $\lambda T \lesssim \tau_0^{-1}$. A similar effect is produced by weak three-dimensional hopping at low temperatures.

IV. DISCUSSION

A. Experiments in $La_{2-x}Sr_xCuO_4$

The structure shown in Figs. 4–6 is similar in magnitude, temperature, and energy dependence to that observed in neutron scattering in $La_{2-x}Sr_xCuO_4$. The spectra weight $\int d\mathbf{q}\,\chi''$ ($\mathbf{q},\omega=10$ meV) in the peaks near (π,π) is calculated to be $\sim 0.4\mu_B^2$ eV^{-1} (using a mass $m^*=5$), which is somewhat below the range of the experimental estimate[10] of $\sim 1-2\mu_B^2$ eV^{-1} in $La_{2-x}Sr_xCuO_4$. By adjusting x_{vh} to a doping level of 5%, our parameters yield peak positions comparable to experiment. This is not in itself remarkable, because the value of δQ is fixed by the vagaries of the band structure. But we note that the peaks *sharpen* as x increases, as in experiment.[10] This is produced in our model by the enhanced nesting as $x\rightarrow x_{sq}$. The evolution of a relatively broad peak at π,π in $La_{1.95}B_{0.05}CuO_4$ (Ref. 7) to incommensurate peaks in $La_{2-x}Sr_xCuO_4$ (Refs. 9 and 10) at $x=0.075$ and $x=0.15$, which become sharper at higher doping, is a strong indication of the Fermi-surface nature of the features. These features are unremarkable in a band picture, but are difficult to obtain in a model which depends entirely on strong magnetic correlations to produce the structure in momentum space. That the scattering derives from itinerant carriers is further supported by the opening of a gap in the superconducting state[10] (see below). Finally, in all these sets of data, there is strong evidence that the characteristic scale for the fluctuation spectrum is set by k_BT, which is natural in the MFL picture, but accidental in other models. The peaks broaden dramatically with temperature and frequency on low-energy scales; a simple band picture cannot account for this by itself.

Comparison with the NMR results is more problematic, partly because this system has not been so carefully studied as $YBa_2Cu_3O_7$. We have also to make a specific choice of orbitals and how they relate to the band structure—implying that we take the prescription of orbitals in Eq. (4) seriously, rather than just providing a parametrization of the Fermi surface. Nevertheless, gross features (the enhancement, and T dependence of $^{63}T_1^{-1}$) match quite well to experiment.

The calculated relaxation rates for Cu are large and comparable to experiment (small by roughly a factor of 2), but the anisotropy of $^{63}T_1$ is too small. As the Knight shifts are not known accurately for this compound we cannot yet say whether the failure to obtain the correct anisotropy represents a serious flaw. The ratio of 10–20 between the Cu and O relaxation rates is also reasonably close to experiment. The non-Korringa behavior of $^{17}T_1^{-1}$ is in disagreement with the only published measurements[33] in $La_{2-x}Sr_xCuO_4$ and $La_{2-x}Ca_xCuO_4$ with $x\sim 0.15$. However, more recent measurements on $La_{2-x}Sr_xCuO_4$ (Ref. 34) and La_2CuO_{4-y} (Ref. 35) show some deviations from the Korringa law for $^{17}T_1$, but the detailed behavior is not unambiguously established. In our calculations, we find $\chi'(0,0)$ to be almost temperature independent; there is no "spin gap" in our model. This is in agreement with experiments on the "best" (i.e., highest T_c) $YBa_2Cu_3O_7$ and $La_{1.85}Sr_{0.15}CuO_4$ samples. A susceptibility increasing with T at low temperature is observed most clearly in the less metallic materials, is outside the scope of our model, and will require extra physics.[36]

The quantitative underestimate of both the NMR relaxation rate and the magnitude of the measure spin susceptibility near (π,π) then indicates a magnetic enhancement of $\chi''(\mathbf{q},\omega)$ in the range of 2–5; and thus an enhancement of $\mathrm{Re}[\chi(\mathbf{q}\approx(\pi,\pi))]$ of 1.5–2.5. This does not suggest that the $La_{2-x}Sr_xCuO_4$ system near $x=0.15$ is close to a magnetic instability.

B. Experiments in $YBa_2Cu_3O_7$

We have been at pains to point out how sensitive our results are to details of band structure, and so we cannot use the present results for $YBa_2Cu_3O_7$. A few comments are, however, in order.

$YBa_2Cu_3O_7$ has undoubtedly a more complex Fermi surface, at least because of a significant hybridization between the two (equivalent) planes within the unit cell. Some band-structure calculations[37] have produced a Fermi surface rotated by 45 degrees from that in $La_{2-x}Sr_xCuO_4$, and this has been claimed to be in agreement with spectroscopic evidence.[38–40] Such a rotated Fermi surface would give rise to peaks in the fluctuation spectrum far from π,π, and this led Zha, Si, and Levin[41] to suggest that a moderate antiferromagnetic coupling

would be needed to restore the spectral weight to its rightful place.

The most recent and complete photoemission measurements[40] show very clear dispersion of bands in $YBa_2Cu_3O_7$ where they are clearly of planar character. In those directions, which are supposed to match the "rotated" Fermi surface, there is no clear dispersion and only an edge at the Fermi energy, such as might come about from a disordered band of states on the chains. We do not find convincing evidence here for the claimed rotation of the Fermi surface. If the rotation of the FS is present, it must derive from a complicated interplay of many orbitals other than those we have in our model Hamiltonian, and it is thus not appropriate to use a three-band model to compare with NMR, which depends strongly on the orbital character. Whether present or not, the greater complexity of the Fermi-surface topology will probably reduce the nesting features, and thus reduce the calculated relaxation rates; indeed the value of $^{63}T_1^{-1}$ is 2–3 times smaller in $YBa_2Cu_3O_7$ than in $La_{2-x}Sr_xCuO_4$, and the deviation from Korringa less dramatic. Neutron-scattering measurements on $YBa_2Cu_3O_7$ show broad features at the commensurate point,[11] which are (especially in fully oxygenated material) much less intense than the peaks observed in $La_{2-x}Sr_xCuO_4$. In $YBa_2Cu_3O_7$ however, the Korringa law for $^{17}T_1^{-1}$ is well established.[2] Our two-dimensional model will naturally give non-Korringa behavior for both O and Cu sites, even if the peak in the fluctuation spectrum is mostly at the commensurate value [compare Figs. 4(a) and 9(a)]; the susceptibility always has a line of singularities. It is possible that three-dimensional hopping (see below) can preferentially destroy the singular behavior everywhere except the zone corner—it is most robust here because of the proximity to the saddle point—and thus rescue the Korringa law for O, while leaving $^{65}T_1$ relatively untouched. We also do not have strong temperature dependence to $\mathrm{Re}[\chi]$ even at large momentum; thus it will be difficult for this model to reproduce the recently observed temperature dependence of T_2.[42]

C. Effects of superconductivity, three dimensionality

We do not present here calculations for the superconducting state, although it is very easy to guess the qualitative features. In an *s*-wave superconductor, and assuming no magnetic interactions, the spin-fluctuation spectrum will develop a gap of 2Δ. Because the quasiparticle lifetime is presumably also produced by electronic scattering, it must therefore become very long at low frequencies $\omega \ll 2\Delta$ and temperatures $T \ll T_c$.[43] Consequently, for energy transfers $2\Delta < \omega < 4\Delta$ the spin fluctuations will be present but *unbroadened* by lifetime effects, which will return on higher energy scales $\omega \gg 4\Delta$. These lifetime effects are most visible in long-wavelength probes (optical and thermal conductivity) but they will have weaker effects at large momentum, more pronounced if nesting plays a role. If the superconducting state is gapless (either from nonzero angular momentum pairing or via pairbreaking) the lifetime effects will be less pronounced.

The divergence in the low-frequency $\chi''(\mathbf{q},\omega)/\omega$ at $2k_F$ is a special feature of two dimensions. While interlayer hopping is weak in the cuprates, it is not zero. At low temperatures, the cutoff of the singularity will be given not by $\mathrm{Im}(\Sigma)$ but by $v_F\delta k_F$, where v_F is the (planar) Fermi velocity and δk_F the maximum dispersion of the two-dimensional Fermi wave vector in the perpendicular direction. Within resolution, this has not been observed in the neutron-scattering experiments in $La_{2-x}Sr_xCuO_4$. This is as expected, because $La_{2-x}Sr_xCuO_4$ is indeed very anisotropic, with a recent measurement of the plasmon in the *c*-axis direction showing that the dispersion is less than the superconducting gap.[27] Note that the anisotropy of the plasma frequency is much larger than predicted by LDA band-structure calculations, which provides additional evidence for the highly correlated nature of the "bands" in $La_{2-x}Sr_xCuO_4$.

Three-dimensional behavior is clearly seen in transport measurements in $YBa_2Cu_3O_7$ above T_c,[44] and the average mass anisotropy is lower than in $La_{2-x}Sr_xCuO_4$. Three dimensionality will necessarily move toward restoration of the linear T dependence for T_1^{-1}, but possibly more strongly for some nuclei than others, depending (again) on details of the band structure.

D. Comparison with other models

There are a number of different models for the magnetic behavior which rely on itinerant carriers and therefore have some features in common with our description. The major difference between our approach and many others is that we have given a description in terms of *noninteracting* but heavily renormalized quasiparticles which do not form a Fermi liquid.

In antiferromagnetic fluctuation models, temperature dependence arises from proximity to an AF instability (i.e., exchange enhancements).[20–22] This is especially enhanced when there is nearly perfect nesting.[24] Such models have strong enhancements in both the real and imaginary parts of the susceptibility; both the static susceptibility

$$\mathrm{Re}[\chi(\mathbf{q},0)]=\int_0^\infty d\omega \mathrm{Im}[\chi(\mathbf{q},\omega)]/\omega$$

and the static structure factor

$$S(\mathbf{q})=\int_0^\infty d\omega[1+n(\omega)]\mathrm{Im}[\chi(\mathbf{q},\omega)]$$

will diverge at the AF instability for the appropriate $\mathbf{q}$. In the paramagnetic phase, there is a low-energy cutoff to the fluctuation spectrum, which means that the properties will be those of a Fermi liquid on a low enough energy scale. In our picture neither the static susceptibility nor the static structure factor is necessarily strongly enhanced. Although weak enhancements (~ 2) are not excluded by our analysis, the correlation length [defined from $S(\mathbf{q})$] in our picture is not long. Another viewpoint is based on bands derived from a mean-field analysis of the $t-J$ model,[45,46] although spin-fluctuation effects [in particular a random-phase-approximation (RPA) -like) renormalization of the susceptibility] were found necessary.

A different approach is based on a proximity to a nearly localized state, which has been argued[23] to lead to a crossover at low temperatures from coherent to incoherent band motion (and which is therefore also a Fermi liquid at low temperatures). This picture does require a very considerable band narrowing to place the coherence temperature in the range of a few hundred degrees. Magnetic fluctuations can also be incorporated in the renormalized bands, and have been suggested to be important in $YBa_2Cu_3O_7$ but not $La_{2-x}Sr_xCuO_4$.[41] Zha, Si, and Levin have used a renormalized band structure and small to moderate (q dependent) magnetic coupling to calculate a RPA susceptibility. They do not include self-energy effects, which we have focused on. While at low temperatures and low frequencies their results are those of a FL, at frequencies or temperatures comparable to or greater than the separation of the chemical potential from the Van Hove singularity, features in the band structure are apparent. In particular, there are peaks in the calculated $S([\pi,\pi],\omega)$ at an energy corresponding to excitation to this edge. They have argued[41] that this feature is responsible for the observed ω/T scaling in $La_{1.95}Ba_{0.05}CuO_4$ (at $x=0.05$, close to x_{vh}), and will lead to deviations in $YBa_2Cu_3O_7$ [where there is a gap in the spectrum at (π,π)]. All of the band-structure effects are present in our calculations, but sharp features at nonzero frequency are not present, owing to the lifetime broadening of the carriers. The approximate scaling between ω and T in Fig. 7 has its origin principally in the self-energy, while the momentum dependence arises from band structure.

The distinction between Fermi-liquid (FL), marginal-Fermi-liquid (MFL), and nearly antiferromagnetic-Fermi-liquid (AFL) behavior is shown in Figs. 10–12. Figure 10 compares the energy dependence of $S(q,\omega)$ for a FL and MFL, with identical band parameters. The oscillator strength in the FL grows linearly with frequency, while for the MFL it is relatively flat, as we saw in Fig. 7. The difference between the two models in terms of temperature dependence at low frequency is less dramatic, as shown in Fig. 11, although the similarity is misleading as will be seen clearly in Fig. 12. In both cases, the singularity in $\chi''(\mathbf{q},\omega)$ is rounded out at finite temperatures, although more rapidly in the MFL case. Here we have also shown the temperature dependence of $\mathrm{Re}[\chi(q,\omega=0]$; in both cases the temperature dependence is weak, because the $T=0$ results is only a cusp. This figure also serves to show that the effect of the MFL self-energy is to reduce the static susceptibility from the noninteracting value, here by roughly a factor of 2. The final comparison shown in Fig. 11 is to a phenomenological model of nearly antiferromagnetic spin fluctuations with a temperature-dependent correlation length ξ.[5,6] For a simple mean-field model of the fluctuations, one has

$$\chi' \propto \xi^2/[1+(q-Q)^2\xi^2]\ , \tag{6a}$$

$$\lim_{\omega\to 0}\chi''/\omega \propto (\chi')^2\ . \tag{6b}$$

To facilitate comparison, we have chosen a value of the incommensurate Q to match the FL and MFL models, and fixed the width of the peak to be in approximate agreement by varying the temperature dependence of ξ.

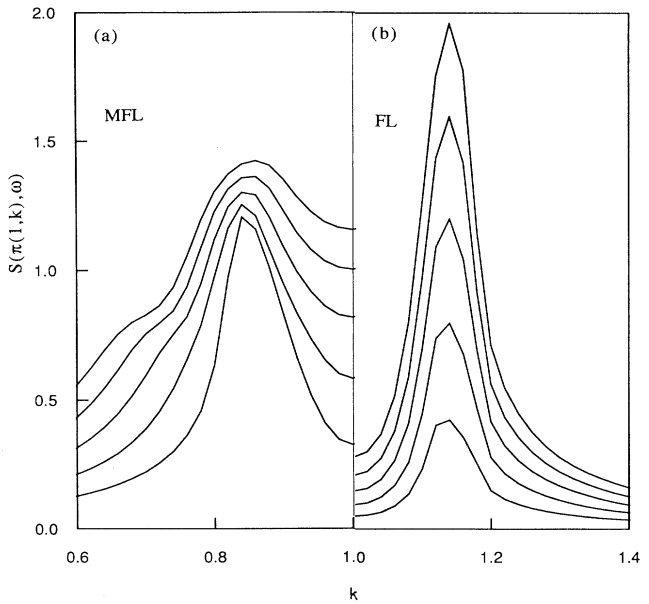

FIG. 10. Spectral function $S(\mathbf{q},\omega)$ along $\mathbf{q}=\pi(1,x)$ with $\varepsilon=1.2$ eV, $t=-1.5$ eV, $t'=0.3$ eV, and $n=0.43$ ($x=0.14$) $\lambda=0.3$, $\omega_c=1$ eV, and $m^*=5$ at $T=20$ K, and energies $\omega=(3,6,9,12,15)$ meV. The left panel (a) uses the MFL form of the self-energy. For comparison the right panel (b) is the conventional Fermi liquid for $\mathrm{Im}(\Sigma)=1$ meV $\cong 10$ K.

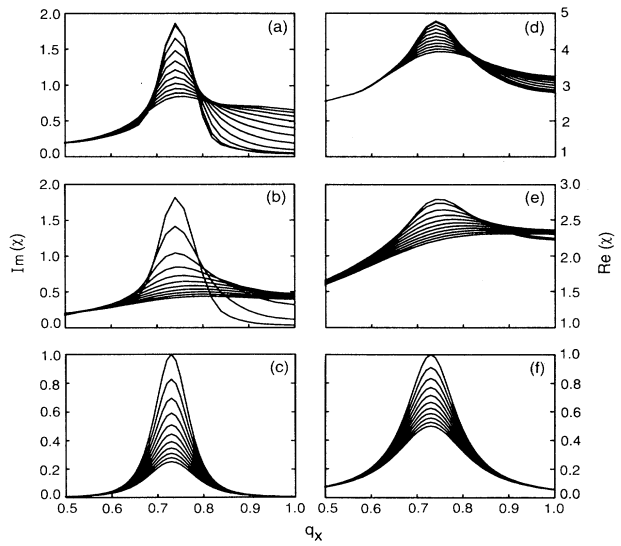

FIG. 11. Susceptibility $\mathrm{Im}[\chi(q=\pi(1,q_x)),\omega=2$ meV] [left panels, (a)–(c)] and $\mathrm{Re}[\chi(q=\pi(1,q_x)),\omega=0]$ [right panels, (d)–(f)] for a FL (a)–(d), MFL (b), (e), and AFL (c), (f), for a set of temperatures $T=0.002, 0.005, 0.010, 0.015, \ldots, 0.050$ eV. For the FL and MFL, parameters are $\varepsilon=1.2$ eV, $t=-1.5$ eV, $t'=0.5$ eV, $m^*=5$, with $\omega_c=1$ eV, $\lambda=0.3$ (MFL) and $\mathrm{Im}(\Sigma)=2$ meV (FL). For the AFL, the susceptibility is described by Eq. (6), and we used $\xi(T)^{-2}=\xi_0^{-2}(1+T/T_0)$ with $\pi\xi_0=15$ and $T_0=0.05$ eV.

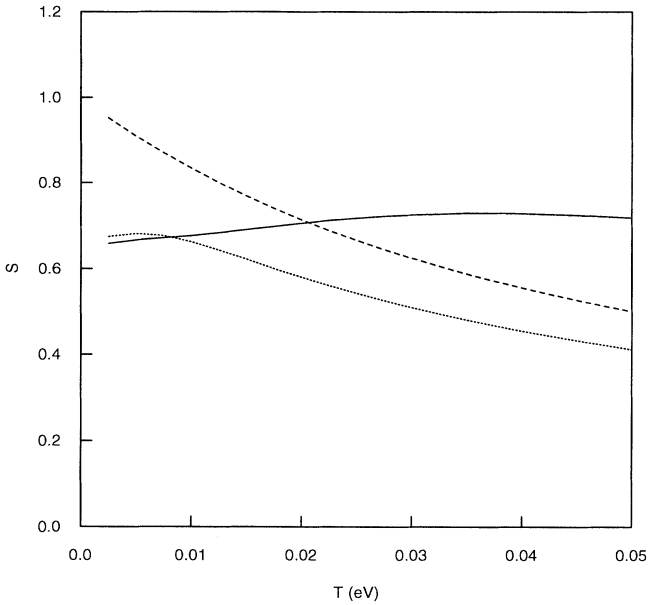

FIG. 12. Low-frequency local spectral function $S=\lim_{\omega\to 0}\sum_q \chi''(q,\omega)/\omega$ for the three models of Fig. 11: FL (solid line), MFL (dotted line), and AFL (dashed line). The relative scales of FL and MFL curves is correct, that of the AFL curve is arbitrary.

In the AFL case, both real and imaginary parts of the susceptibility are strongly dependent on temperature. The temperature dependence of $\mathrm{Re}(\chi)$ is the signature of proximity to a magnetic transition.

Finally, Fig. 12 shows the local susceptibility $S=\sum_q \chi''(q,\omega)/\omega$ for the three cases, which is approximately the contribution of the fluctuations to Cu NMR relaxation rate $1/T_1T$. Notice that this quantity has almost no temperature dependence in the FL despite the superficial similarity of Figs. 11(a) and 11(b). The difference between FL and MFL is that in the former case, the effect of nonzero temperature is simply to redistribute weight to different momenta as the Fermi surface is smeared. If the density of states were uniform, the FL model would have no temperatue dependence of the momentum-averaged susceptibility. The self-energy in the MFL contributes to a suppression of the imaginary part of the susceptibility for momenta below $2k_F$, which is not entirely counterbalanced by the growth at momenta above $2k_F$. The net effect is that the MFL looks much like a model of a nearly antiferromagnetic Fermi liquid with a long and temperature-dependent correlation length. The distinction between MFL and AFL is seen most clearly in their differing predictions for the real part of the susceptibility.

Returning to a microscopic point of view, it has been suggested that Van Hove singularities or Fermi-surface nesting can feed back on themselves to give the MFL scenario.[47,24,48] Figure 8 makes it clear that only a very modest temperature dependence in physical quantities can be obtained from the bare density of states. With Coulomb interactions (V_q) included, it might appear that the feedback of quasiparticles interacting with the polarizability of Eq. (1) can lead to the MFL prescription, since in leading order, $\Sigma''(\omega\to 0)\propto \sum_q V_q\chi''(\mathbf{q},\omega)\propto T_1^{-1}$. However, unless there is a nesting singularity (which would be expected only at a special composition), the temperature dependence of the NMR rate is at most $T^{1/2}$, and we will not obtain self-consistently the MFL results. Moreover, there is a natural low-energy cutoff for the restoration of Fermi-liquid behavior controlled by the difference of the chemical potential from perfect nesting.[47] Furthermore, the self-energy here is a strong function momentum, which is not obviously consistent with tunneling measurements.[49] Finally, a MFL model which contains a singularity in $\chi'(q,\omega)$ (e.g., from a perfect nesting) would be very likely to undergo a phase transition to charge or spin-density wave states, or is otherwise unstable to higher-order terms.[50]

We have stressed the Fermi-surface contribution to χ'', but NMR measurements are also sensitive to any temperature-dependent background proportional to $\mathrm{Im}(\Lambda)$ as in the original MFL picture, with $\Lambda=1+\lambda\ln(x/\omega_c)+i\lambda\pi x/T$, where $x=\max(\omega,T)$ and $qv_F>\omega$.[51] The assumed ω/T form combined with the Knight-shift estimates above would then give an additive and T-independent contribution to T_1^{-1} of about 100 sec^{-1} on O, and 150 sec^{-1} on Cu. The O contribution is comparable to or larger than the band-structure piece in Fig. 9; the failure to observe such a large non-Korringa term on O (in $YBa_2Cu_3O_7$) throws in doubt the presence of a MFL vertex in the spin channel, at least using the conventional hyperfine Hamiltonian.[52]

V. CONCLUSION

In conclusion, we have found that a simple band-structure model of $La_{2-x}Sr_xCuO_4$, together with anomalous self-energy corrections and a moderate mass enhancement can give a reasonable account of the energy and momentum dependence of the magnetic structure factor at low frequencies, as measured by neutron scattering. We require neither strong magnetic interactions, nor a polarizability of the form originally suggested in MFL (Ref. 15) to account for the data. We do not require strong exchange enhancements of the type found in the insulating cuprates; nevertheless, our results parallel the phenomenological model of Millis, Monien, and Pines[5] because the peaks in $S(q)$ broaden with increasing temperature. Unlike other models,[20,23] there is no temperature scale below which Fermi-liquid behavior is restored. The only length scale in our model is the mean free path for the quasiparticles near the Fermi level, and it is this which controls the visibility of the peaks in $S(q,\omega)$. The principal experimental distinction between our model, and models which require large magnetic coupling, is in the real part of the susceptibility $\chi'(\mathbf{q})$, or in the instantaneous structure factor $S(\mathbf{q})$.

Itinerancy of the carriers, and a corresponding band structure, need not correspond to the simple picture, e.g., that given by LDA. For example, it is clear that in the t-J model at a moderate doping there appears a well-defined dispersion for quasiparticles.[53] Series expansion

techniques indicate that the structure factor has a peak on the zone boundary at momenta not far from that expected in an unrenormalized band.[54] All that is required is a large Fermi surface, and the appropriate strong renormalization of the quasiparticle lifetime.

Our results are somewhat less successful when compared to NMR measurements. Since neutron scattering is sensitive to sharp features in momentum space, and NMR measures local properties (averages in momentum space) it is possible that there are broad features which dominate the NMR (and correspond to real magnetic interactions) but are difficult to observe by spectroscopic techniques. Nevertheless, we believe the anomalous T_1^{-1} on Cu is associated with the emergence of the peaks in $S(q,\omega)$ below 150 K in $La_{1.85}Sr_{0.15}CuO_4$. In addition, we predict non-Korringa behavior for the NMR rate on oxygen in this compound.

ACKNOWLEDGMENTS

We acknowledge several stimulating discussions with B. Batlogg, R. Birgeneau, K. Levin, A. Millis, H. Mook, S. Shastry, C. M. Varma, and R. E. Walstedt. J. Z. acknowledges support by the Foundation of Fundamental Reserach on Matter (FOM), which is sponsored by the Netherlands Organization for the Advancement of Pure Research (NWO). H.M. acknowledges support under NSF Grant No. PHY-04035.

[1]R. E. Walstedt *et al.*, Phys. Rev. B **38**, 9299 (1988).
[2]P. C. Hammel *et al.*, Phys. Rev. Lett. **63**, 1992 (1989); R. E. Walstedt and W. W. Warren, Jr., Science **248**, 1082 (1990).
[3]F. Mila and T. M. Rice, Physica C **157**, 561 (1989); Phys. Rev. B **40**, 11 382 (1989).
[4]B. S. Shastry, Phys. Rev. Lett. **63**, 1288 (1989).
[5]A. J. Millis, H. Monien, and D. Pines, Phys. Rev. B **42**, 167 (1990).
[6]A. J. Millis and H. Monien, Phys. Rev. B **45**, 3059 (1992).
[7]S. M. Hayden *et al.*, Phys. Rev. Lett. **66**, 821 (1990).
[8]B. Keimer *et al.*, Phys. Rev. Lett. **67**, 1930 (1991).
[9]S.-W. Cheong *et al.*, Phys. Rev. Lett. **67**, 1791 (1991).
[10]T. E. Mason, G. Aeppli, and H. A. Mook, Phys. Rev. Lett. **68**, 1414 (1992).
[11]J. Rossat-Mignod *et al.*, Physica B **169**, 58 (1991), and references therein; J. M. Tranqada, in Proceedings of University of Miami Workshop on Electronic Structure and Mechanisms for High-T_c Superconductivity, 1991, edited by J. Ashkenazy and G. Vezzoli (Plenum, New York, in press).
[12]T. Takahashi *et al.*, Phys. Rev. B **42**, 381 (1990).
[13]H. Hagighi *et al.*, Phys. Rev. Lett. **67**, 382 (1991); L. P. Chan *et al.*, Phys. Rev. Lett. **67**, 1351 (1991).
[14]C. G. Olsen *et al.*, Phys. Rev. B **42**, 381 (1990).
[15]C. M. Varma *et al.*, Phys. Rev. Lett. **63**, 1996 (1989); **64**, 497(E) (1990).
[16]G. Kotliar *et al.*, Europhys. Lett. **15**, 655 (1991).
[17]For a discussion, see, P. B. Littlewood (unpublished).
[18]Preliminary results were presented in P. B. Littlewood, J. Zaanen, G. Aeppli, and H. Monien (unpublished); H. Monien (unpublished).
[19]R. J. Jelitto, Phys. Status Solidi B **147**, 391 (1988).
[20]N. Bulut, D. Hone, D. J. Scalapino, and N. E. Bickers, Phys. Rev. B **41**, 1797 (1990).
[21]L. Chen, C. Bourbonnais, T. Li, and A.-M. S. Tremblay, Phys. Rev. Lett. **66**, 369 (1991); P. Benard, L. Chen, and A.-M. S. Tremblay, Phys. Rev. B **47**, 589 (1993).
[22]V. Barzykin and L. P. Gor'kov (unpublished).
[23]J. P. Lu, Q. Si, J. H. Kim, and K. Levin, Phys. Rev. Lett. **65**, 2466 (1990); Physica C **179**, 191 (1991); Y. Zha, Q. Si, and K. Levin (unpublished); Q. Si *et al.* (unpublished).
[24]J. Ruvalds, C. T. Rieck, J. Zhang, and A. Virosztek, Science **256**, 1664 (1992).
[25]See also Benard *et al.* (Ref. 21).
[26]W. E. Pickett, H. Krakauer, and R. E. Cohen, Physica B **165** and **166**, 1055 (1990).
[27]K. Tamasaku, Y. Nakamura, and S. Uchida, Phys. Rev. Lett. **69**, 1455 (1992).
[28]A. K. McMahan, J. F. Annett, and R. M. Martin, Phys. Rev. B **42**, 6268 (1990); A. J. Freeman, J. Yu, and C. L. Fu, Phys. Rev. B **36**, 7111 (1987); M. S. Hybertsen (private communication).
[29]For $q\rightarrow 0$ quantities, we must use the bare density of states, i.e., $\Sigma\rightarrow 0$, $\Lambda\rightarrow 1$ in Eq. (1).
[30]See, e.g., B. Batlogg, Physica B **169**, 7 (1990).
[31]S. E. Barrett *et al.*, Phys. Rev. B **41**, 6283 (1990); M. Takigawa *et al.*, *ibid.* **39**, 7371 (1989).
[32]T. Imai, J. Phys. Soc. Jpn. **59**, 2508 (1990).
[33]L. Reven *et al.*, Phys. Rev. B **43**, 10 466 (1991).
[34]R. E. Walstedt *et al.* (unpublished).
[35]P. C. Hammel *et al.* (unpublished).
[36]A. J. Millis and H. Monien, Phys. Rev. B **45**, 3059 (1992).
[37]J. J. Yu, S. Massidda, A. J. Freeman, and D. D. Koehling, Phys. Lett. A **122**, 203 (1987).
[38]A. J. Arko *et al.*, Phys. Rev. B **40**, 2268 (1989).
[39]J. C. Campuzano *et al.*, Phys. Rev. Lett. **64**, 2308 (1990).
[40]R. Liu, B. W. Veal, A. P. Paulikas, J. W. Downey, P. J. Kostic, S. Fleshler, U. Welp, C. G. Olson, X. Wu, A. J. Arko, and J. J. Joyce (unpublished).
[41]Y. Zha, Q. Si, and K. Levin (unpublished).
[42]T. Imai *et al.* (unpublished).
[43]P. B. Littlewood and C. M. Varma, Phys. Rev. B **46**, 405 (1992).
[44]M. Charalambous, J. Chaussy, and P. Lejay, Physica B **169**, 637 (1991).
[45]T. Tanamoto, K. Kuboki, and H. Fukuyama, J. Phys. Soc. Jpn. **60**, 3072 (1991); T. Tanamoto, H. Kohno, and H. Fukuyama (unpublished).
[46]D. R. Grempel and M. Lavagna (unpublished).
[47]A. Virosztek and J. Ruvalds, Phys. Rev. B **42**, 4064 (1990); J. Ruvalds and A. Virosztek, *ibid.* **43**, 5498 (1991).
[48]C. C. Tsuei *et al.*, Phys. Rev. Lett. **65**, 2724 (1990); D. M. Newns *et al.*, Phys. Rev. B **38**, 7033 (1988).
[49]P. B. Littlewood and C. M. Varma, Phys. Rev. B **45**, 12 636 (1992).
[50]G. Zimanyi and K. S. Bedell, Phys. Rev. Lett. **66**, 228 (1991); (unpublished).
[51]A. Ruckenstein and C. M. Varma (unpublished).
[52]We note that optical absorption and Raman-scattering probe $q\sim 0$, where there is no anomalous vertex. NMR is the only probe which is sensitive to a local contribution to the susceptibility.
[53]W. Stephan and P. Horsch, Phys. Rev. Lett. **66**, 2258 (1991).
[54]R. Singh and R. L. Glenister (unpublished).